Synopsis of thesis entitled

Development of Stabilized Palladium Nanocatalysts Based on Heteropoly acids and Their Applications in some Organic Transformations

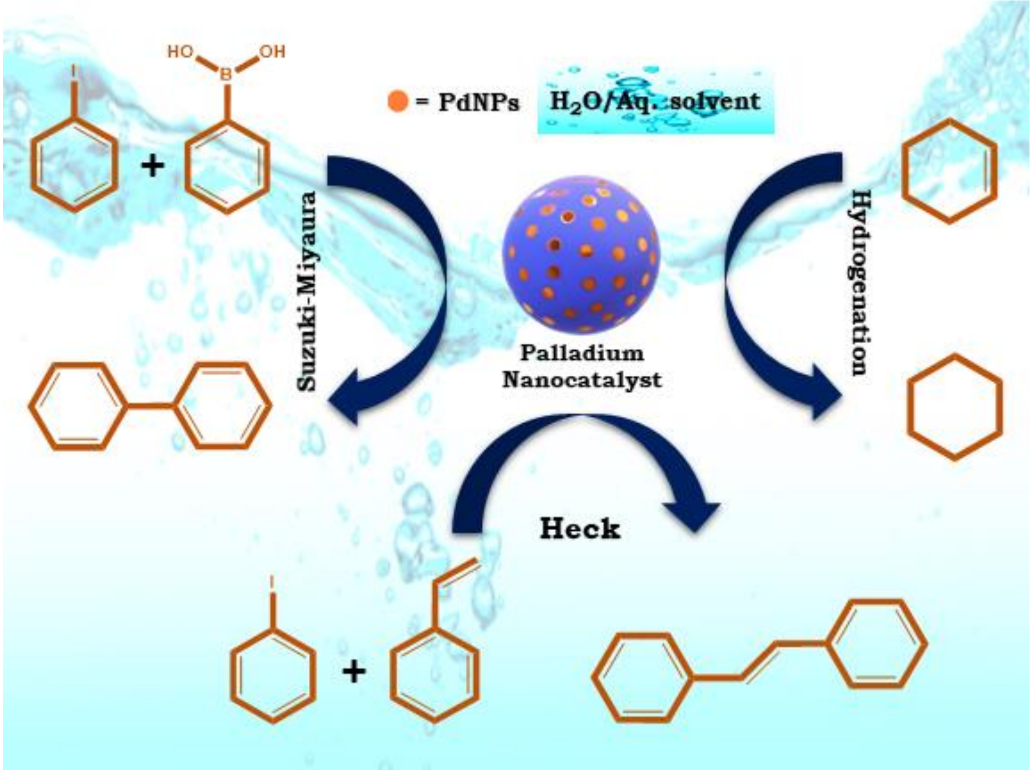

To be submitted to
The Maharaja Sayajirao University of Baroda

For the Degree of

DOCTOR OF PHILOSOPHY
In
CHEMISTRY

By

Anish Patel

Department of Chemistry
Faculty of Science
The Maharaja Sayajirao University of Baroda
Vadodara, 390 002
INDIA
March, 2020

Introduction

Developing chemical reactions catalyzed by palladium-based materials have gained noble recognition because its unique properties make it intensively investigated, prevalent and permits real exploitation[1] dominantly over Pt, Au, Ir etc. Moreover, its ability to activate and facilitates industrially important molecules without getting incorporated in to the final product is the most considerable factor. However, especially in case of Pd nanoparticles (PdNPs), the associated key issues are the aggregates formation during the catalyst synthesis or the reaction due to its ultra-small size and high surface energy[2, 3]. To overcome the same, different stabilizing agents such as phosphorus base ligands, dendrimers, polyvinyl pyridine, cyclodextrin, surfactants, ionic liquids and carbene complexes, and most of these are highly expensive and toxic organic ligands[3-7].

The use of such ligands can be avoided by the replacement of some other materials, able to stabilize PdNPs into either its lowest oxidation state or highest oxidation state, depending on the noble metal. In advancement to this, polyoxometalates (POMs) are the excellent candidates for the same because they are the unique class of inorganic compounds having discrete metal–oxygen cluster composed of transition metals of group V and VI in high oxidation states and acidic form of them are known as heteropoly acids. They are very fascinating and excellent as stabilizing agent for PdNPs, due to their number of convergent properties such as robust oxoanionic nature, its negative charges, large relative sizes, stability, reducing and encapsulating agent[8-11].

The direct use of POM stabilized PdNPs is often associated with difficult catalyst recovery as POMs are homogeneous in polar solvent[12,13], material deactivation and reduced efficiency in organic transformations. To overcome, a much simpler method is to anchor the such materials with different supports such as inorganic materials, organic polymers, metal organic frameworks (MOFs) and membranes.

The stabilized PdNPs can be designed at molecular level by different synthetic methods as shown in scheme 1.

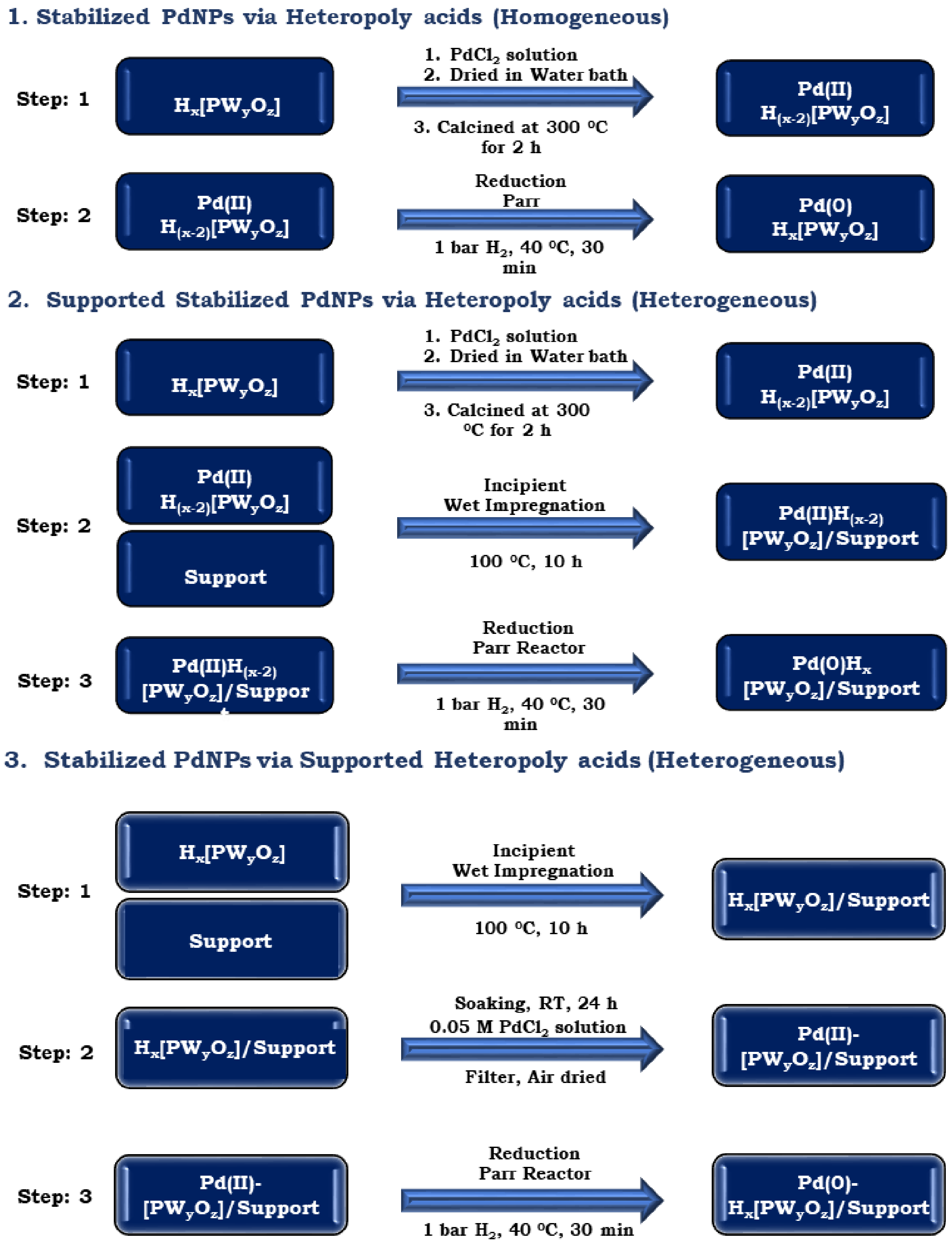

Scheme 1 Designing scheme of stabilized PdNPs at molecular level.

As a catalytic efficiency evaluation, C-C cross coupling (Suzuki-Miyaura and Heck) and hydrogenation reactions were selected due to their great industrial importance. For example, C-C cross coupling are used to synthesize natural products, perfumery intermediates, active pharmaceutical ingredients, advance materials and food products [14]. Whereas, hydrogenation of aromatics and aliphatics provides the precursors for the production of edible fats from liquid oils, petroleum industry, numerous processes involved in the manufacture of gasoline and petrochemical products, pharmaceutical and food industries.

On these lines, the following objectives were proposed.

Objectives of the work

- To design ligand free stabilized Palladium nanoparticles (PdNPs) via heteropoly acids (12-tungstophosphoric acid, mono lacunary tungstophosphate, homogeneous).
- To synthesize metal oxide (ZrO_2, SiO_2) supported stabilized PdNPs via heteropoly acids (HPAs) using different methods.
- To characterize synthesized materials by various techniques such as EDX, FT-IR, TGA, ^{31}P MAS NMR, XPS, Powder XRD, BET Surface Area, SEM, TEM, HRTEM and STEM.
- To use the synthesized materials as catalysts for C-C coupling (Suzuki-Miyaura and Heck) and hydrogenation.
- To study all the reaction parameters such as ratio of substrate to catalysts, temperature, pressure, time and solvent for maximum conversion as well as product selectivity.
- To study reaction mechanism.
- To compare the efficiency of all the catalysts and propose the best catalyst.

The work is divided into two parts based on synthesis

Part A:

Chapter 1: Stabilized PdNPs by 12-tungstophosphoric acid: Synthesis, characterization and applications for SM, Heck and hydrogenation

Chapter 2: Zirconia Supported Stabilized PdNPs by 12-tungstophosphoric acid: Synthesis, characterization and applications for SM, Heck and hydrogenation

Chapter 3: Zirconia Supported Stabilized PdNPs by mono lacunary tungstophosphate: Synthesis, characterization and applications for SM, Heck and hydrogenation

Part B:

Chapter 1: Stabilized PdNPs by zirconia supported 12-tungstophosphoric acid: Synthesis, characterization and applications for SM and hydrogenation

Chapter 2: Stabilized PdNPs by zirconia supported mono lacunary tungstophosphoric acid: Synthesis, characterization and applications for SM, Heck and hydrogenation

Annexure: Silica encapsulated Stabilized PdNPs by 12-tungstophosphoric acid: Synthesis, characterization and applications for SM, Heck and hydrogenation

Part A:

Chapter 1: Stabilized PdNPs by 12-tungstophosphoric acid: Synthesis, characterization and applications for SM, Heck and hydrogenation

Palladium tungstophosphate was synthesized by direct method as reported in the literature[15] with modification. 1 g of PW_{12} was dissolved in minimum amount of distilled water followed by the addition of a stoichiometric amount of aqueous $PdCl_2$ (58.6 mg) solution dropwise. The resulting mixture was aged for 1 h at 80 °C and the excess water was evaporated to dryness on the water bath. The resulting material was oven dried at 120 °C overnight, calcined at 300 °C for 2 h, obtained brown colored $Pd(II)PW_{12}$, finally treated under 1 bar H_2 pressure at 40 °C for 30 min in Parr reactor, obtained (black colored) material was designated as $PdPW_{12}$.

Characterization

The synthesized materials were characterized by elemental analysis, TGA, BET, FT-IR, ^{31}P MAS NMR, powder XRD, XPS and TEM.

The gravimetric analysis of Pd (3.52 wt %) and W (74.40 wt %) in $PdPW_{12}$ were in good agreement with the theoretical values (3.60 wt % and 74.59 wt % respectively) as well as EDS values (3.46 wt % and 74.87 wt % respectively). TGA of $PdPW_{12}$ showed 0.8 % weight loss, adsorbed water, in the temperature range of 70-150 °C. While, 3.0 % weight loss up to 220 °C, indicating the loss of crystalline water molecules. Besides this, no significant weight loss was observed up to 350 °C, suggesting higher thermal stability of the catalyst.

The characteristic bands for PW_{12} were obtained at 1088, 987, 893 and 800 cm^{-1} corresponding to P–O, W=O and W–O–W stretching respectively. The characteristic bands for $PdPW_{12}$ were observed at 1080, 982, 890 and 795 cm^{-1} corresponding to P−O, W=O, and W−O−W stretching, respectively. Here, no splitting of v(P-O) into 1088 and 1042 cm^{-1} confirm the presence of Pd as a counter ion only[16]. The slight shift in the v(P-O) as compared to $PdPW_{12}$ may be due to the replacing of protons by Pd.

The XRD patterns of PW_{12} and $PdPW_{12}$ catalysts were recorded. The XRD patterns of $PdPW_{12}$ showed all the patterns corresponds to PW_{12}, indicating the retention of PW_{12} structure in the synthesized material.

The XPS of $PdPW_{12}$ confirm the electronic properties of Pd and W. $PdPW_{12}$ showed a high intense peak at 532 eV ($3p_{3/2}$) along with a low intense peaks at 335 eV ($3d_{5/2}$) and 558 eV ($3p_{1/2}$) confirming the presence of Pd(0)[10, 17-19]. However, there was still a small amount of Pd(II) present, as evidenced by corresponding peak at 341.6 eV ($3d_{3/2}$)[20]. This may be because of air oxidation of the surface of Pd(0) during the drying process.

TEM images of the fresh catalyst as well as SAED image indicate the uniform dispersion of Pd(0) in the synthesized material. The dark uniform suspension in the images indicates the presence of very tiny Pd(0) nanoparticles (PdNPs) throughout the morphology without any aggregate formation, confirming the stabilization PdNPs by PW_{12}.

In summary, FT-IR and XRD showed the retention of Keggin unit even after reduction of the catalyst. XPS confirmed the presence of Pd(0) and W(VI). TEM indicated the sole presence of highly dispersed PdNPs over the surface of the catalyst.

To evaluate the efficiency of $PdPW_{12}$ as homogeneous catalyst, SM, Heck and hydrogenation reactions were carried out under experimental conditions up to five catalytic runs (Figure 1). In case of PW_{12}, after reaction completion, the organic layer was extracted by dichloromethane and aqueous layer was recovered for the use of next catalytic run directly. Obtained results show that initially catalyst was active and for consequent runs it gradually decreases for all three reactions. As shown in Figure 1d, during first catalytic run, Pd aggregates were clearly observed in the reaction mixture, indicates the leaching of Pd(0) nanoparticles. Hence, further reaction optimization was not carried out.

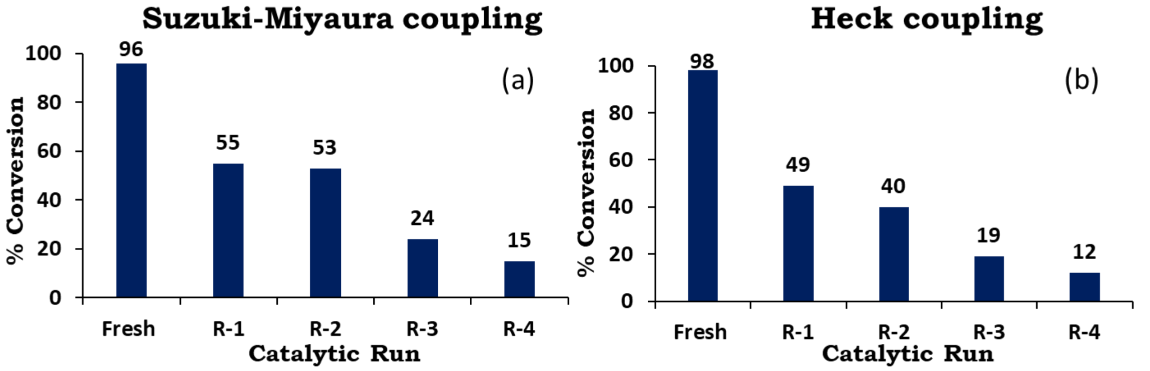

Reaction conditions: Iodobenzene (1.96 mM), PBA (2.94 mM), K_2CO_3 (3.92 mM), Conc. of Pd (3.52×10^{-4} mM), C_2H_5OH: H_2O (3:7 ml), time (30 min), temp. (90 °C).

Reaction conditions: Iodobenzene (0.98 mM), Styrene (1.49 mM), K_2CO_3 (1.96 mM), Conc. of Pd (1.06×10^{-3} mM), DMF:H_2O (3:2) mL, time (6 h), temp. (100 °C).

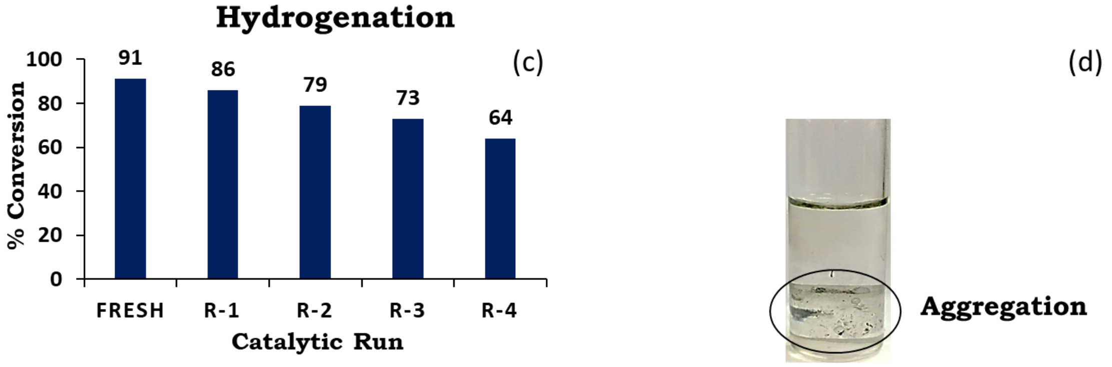

Reaction conditions: Cyclohexene (9.87 mmol), Conc. of Pd (0.015 mol%), H_2O (50) mL, time (4 h), temp. (80 °C) and H_2 Pressure (10 bar).

Figure 1 Catalytic evaluation towards SM, Heck and hydrogenation reactions.

To overcome this problem, the synthesized material was supported on metal oxide supports…

Chapter 2: Zirconia Supported Stabilized PdNPs by 12-tungstophosphoric acid: Synthesis, characterization and applications for SM, Heck and hydrogenation

A series of materials, containing 10-40 % of Pd(II)PW_{12} supported on ZrO_2 was synthesized by incipient wet impregnation method. 1 g of ZrO_2 was impregnated with aqueous solution of Pd(II)PW_{12} (0.1/10-0.4/40 g mL^{-1} of double distilled water) and dried at 100 °C for 10 h and finally treated under 1 bar H_2 pressure at 40 °C for 30 min using Parr reactor. The obtained materials with 10-40 % loading was designated as 10 % $PdPW_{12}/ZrO_2$, 20 % $PdPW_{12}/ZrO_2$, 30 % $PdPW_{12}/ZrO_2$ (Latter, $PdPW_{12}/ZrO_2$) and 40 % $PdPW_{12}/ZrO_2$ respectively.

Characterization

The synthesized materials were characterized by elemental analysis, TGA, BET, FT-IR, ^{31}P MAS NMR, powder XRD, XPS and TEM.

The gravimetric analysis of Pd (3.52 wt %) and W (74.40 wt %) in $PdPW_{12}$ were in good agreement with the theoretical values (3.60 wt % and 74.59 wt % respectively) as well as EDS values (3.46 wt %

and 74.87 wt % respectively). For $PdPW_{12}/ZrO_2$, analytical values for W (17.43 wt %) and Pd (0.80 wt %) were also in good agreement with theoretical values, W (17.21 wt %) and Pd (0.82 wt %).

TGA of $PdPW_{12}$ showed 0.8 % weight loss, adsorbed water, in the temperature range of 70-150 °C. While, 3.0 % weight loss up to 220 °C, indicating the loss of crystalline water molecules. Whereas, $PdPW_{12}/ZrO_2$ showed an initial weight loss of 2.3 % up to 150 °C, indicating the loss of adsorbed water molecules. Besides this, no significant weight loss was observed up to 500 °C, suggesting higher thermal stability of the catalyst.

The BET surface area of ZrO_2 and $PdPW_{12}/ZrO_2$ were found to be 170 $m^2 g^{-1}$ and 202 $m^2 g^{-1}$ respectively. The observed drastic increase in the value of surface area of $PdPW_{12}/ZrO_2$, conforming the reduction of Pd(II) to Pd(0) and in good agreement with the known fact that nanoparticles have higher surface area than the parent one. It is very interesting to note down that in spite of different surface area, the nitrogen adsorption desorption isotherms are almost similar for ZrO_2 and $PdPW_{12}/ZrO_2$, confirming no change in the basic structure.

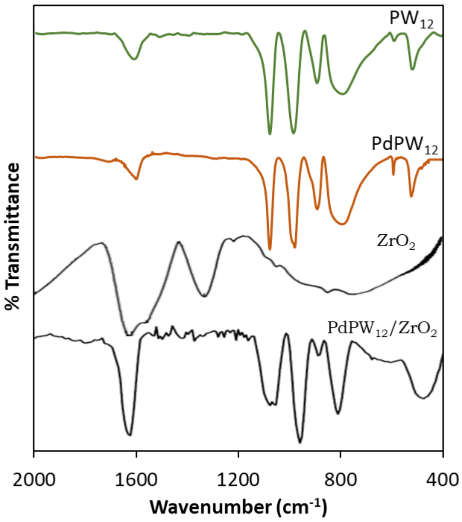

Figure 2 FT-IR spectra.

FT-IR spectra of ZrO_2, TPA, $PdPW_{12}$ and $PdPW_{12}/ZrO_2$ were recorded (Figure 2). ZrO_2 showed two bending vibrations at 1600 and 1370 cm^{-1} for O–H–O and H–O–H vibrations and weak bending vibration of Zr–O–H at 600 cm^{-1}. The characteristic bands for PW_{12} were obtained at 1088, 987, 893 and 800 cm^{-1} corresponding to P–O, W=O and W–O–W stretching respectively. The characteristic bands for $PdPW_{12}$ were observed at 1080, 982, 890 and 795 cm^{-1} corresponding to P−O, W=O, and W−O−W stretching, respectively. Here, no splitting of v(P-O) into 1088 and 1042 cm^{-1} confirm the presence of Pd as a counter ion only[16]. The slight shift in the v(P-O) as compared to $PdPW_{12}$ may be due to the replacing of protons by Pd. The FT-IR spectrum of $PdPW_{12}/ZrO_2$ shows the characteristic bands at 824, 945 and 1056 cm^{-1} corresponding to stretching vibration for W–O–W, W=O and P=O but with significant shift may be due to the change in the environment. The obtained results confirm the supporting of $PdPW_{12}$ onto zirconia.

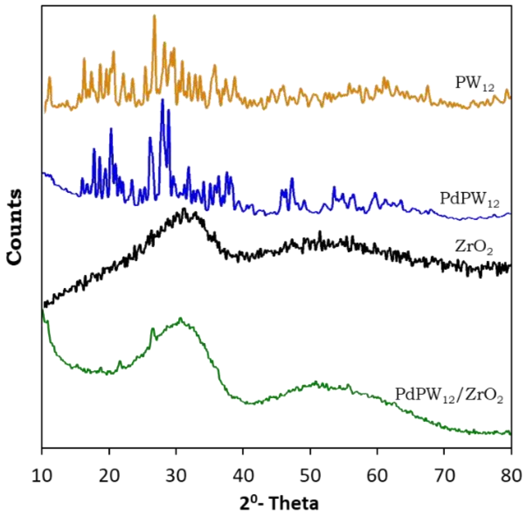

Figure 3 XRD spectra.

The XRD patterns of ZrO_2, PW_{12}, $PdPW_{12}$ and $PdPW_{12}/ZrO_2$ catalysts were recorded (Figure 3). The XRD patterns of ZrO_2 shows the amorphous nature of the support. Whereas, $PdPW_{12}$ showed all the patterns corresponds to PW_{12}, indicating the retention of PW_{12} structure. The XRD pattern of $PdPW_{12}/ZrO_2$ does not show any characteristic diffraction line indicating that a high dispersion of $PdPW_{12}$ in a non-crystalline form on the surface of ZrO_2.

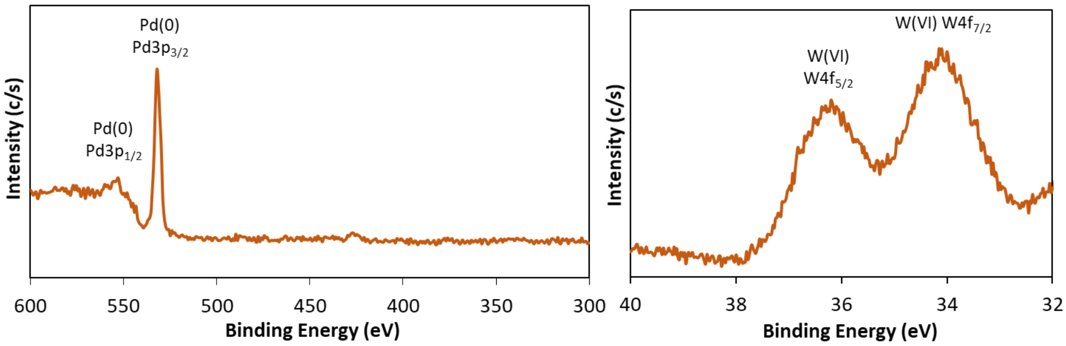

Figure 4 XPS spectra of $PdPW_{11}/ZrO_2$.

The XPS of $PdPW_{12}/ZrO_2$ confirms (Figure 4) the electronic properties of Pd and W. $PdPW_{12}/ZrO_2$ showed a high intense peak at 532 eV ($3p_{3/2}$) along with a low intense peak at 558 eV ($3p_{1/2}$), indicating the presence of the Pd(0) in the encapsulated material. The W4f peak was composed of a well resolved spin orbit doublet (34.45 eV and 36.50 eV for $PdPW_{12}$, 34.38 eV and 36.40 eV for $PdPW_{12}/ZrO_2$ correspond to $W4f_{7/2}$ and $W4f_{5/2}$ respectively), typical of W(VI), in agreement with literature data on Keggin-type POMs[18], confirming no reduction of W(VI) during the synthesis of material. XRD and

XPS confirmed the uniform dispersion of Pd(0), without any sacrifice of PW_{12} structure, over surface of ZrO_2.

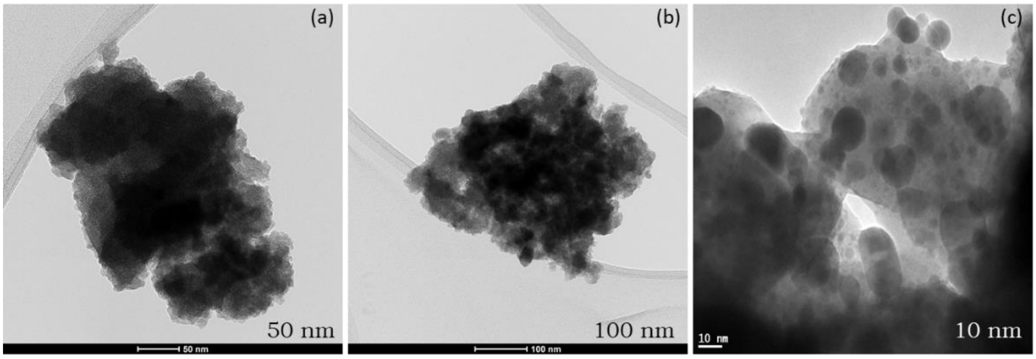

Figure 5 (a & b) TEM and (c) HRTEM images.

TEM and HRTEM images of the fresh catalyst (Figure 5) indicate the non-crystalline and uniform dispersion of Pd(0) in the synthesized material. The dark uniform suspension in the amorphous nature of the catalyst indicates the presence of very tiny Pd(0) nanoparticles (PdNPs) throughout the morphology without any aggregate formation, confirming the stabilization PdNPs by PW_{12}.

In summary, FT-IR and XRD showed the retention of Keggin unit even after impregnation soaking and reduction of the catalyst. XPS confirmed the presence of Pd(0) and W(VI). TEM indicated the sole presence of highly dispersed PdNPs over the surface of the catalyst.

Catalytic Activity

SM Coupling

The efficiency of the $PdPW_{12}/ZrO_2$ as catalyst was studied towards the Suzuki-Miyaura (SM) coupling reaction. Iodobenzene was selected as the ideal substrate for the reaction to optimize the different influential reaction parameters such as substrate to catalyst ratio (catalyst amount), time, temperature, base and solvent for highest product conversion (scheme 2).

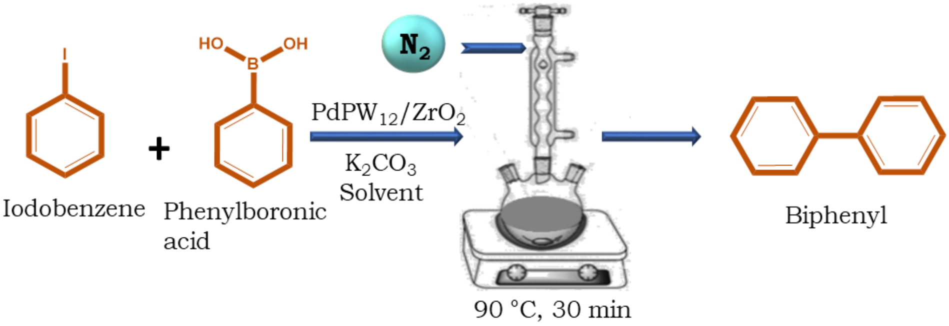

Scheme 2 Suzuki-Miyaura coupling.

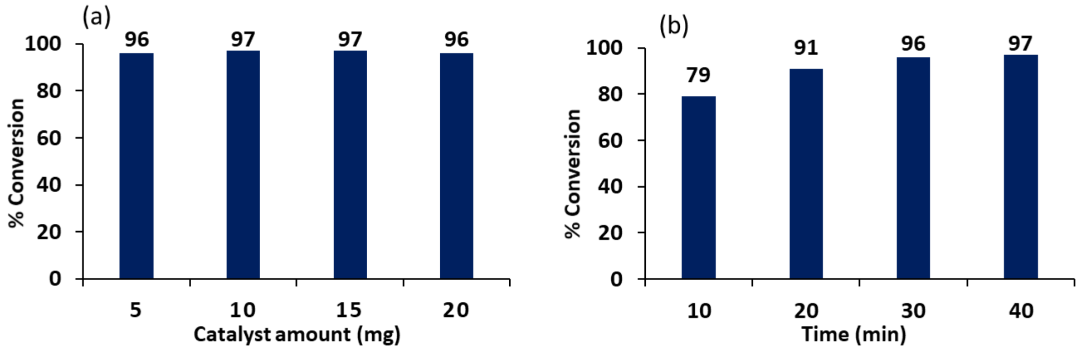

Iodobenzene (1.96 mmol), phenylboronic acid (2.94 mmol), K_2CO_3 (3.92 mmol), EtOH:H_2O (3:7) mL, temperature (90 °C), time (30 min)

Iodobenzene (1.96 mmol), phenylboronic acid (2.94 mmol), catalyst (5 mg), K_2CO_3 (3.92 mmol), EtOH:H_2O (3:7) mL, temperature (90 °C)

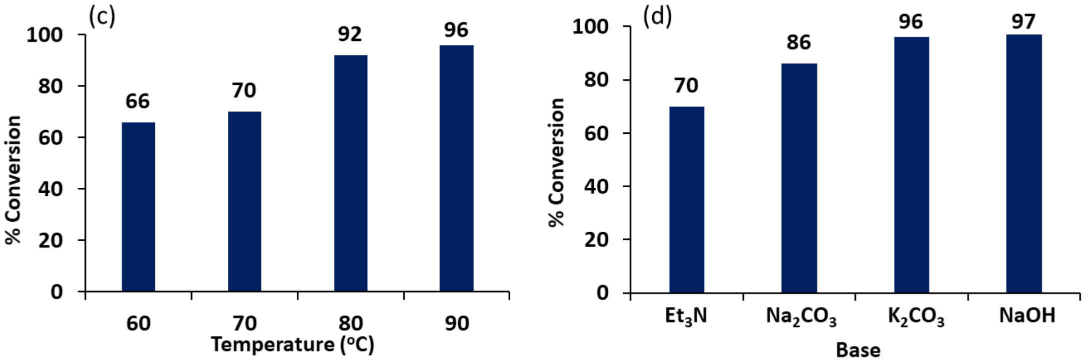

Iodobenzene (1.96 mmol), phenylboronic acid (2.94 mmol), catalyst (5 mg), K_2CO_3 (3.92 mmol), EtOH:H_2O (3:7) mL, time (30 min)

Iodobenzene (1.96 mmol), phenylboronic acid (2.94 mmol), catalyst (5 mg), base (3.92 mmol), EtOH:H_2O (3:7) mL, temperature (90 °C), time (30 min)

Figure 6 Optimization of reaction parameters.

The concentration effect of the Pd(0) on the reaction is shown in Fig 6a. The reaction was carried out by varying the catalyst amount in the range of 5 to 20 mg. The conversion remained unchanged with increase in catalyst amount. This indicates that very low concentration of Pd(0) is sufficient for the maximum % conversion.

The effect of time on catalytic conversion was screened by varying the time from 10 to 40 min as shown in Fig. 6b. The gradual increase was found in % conversion from 10 to 30 min, with further increase in time had no appreciable effect on % conversion. Hence, 30 min time was optimized for the reaction.

The effect of temperature was studied and obtained results are presented in Fig. 6c. The reaction was carried out by varying the temperature range from 50 to 90 °C. It can be seen from the table that with increase in temperature, the % conversion also increases. 96% conversion was obtained at 90 °C. Further, increase in temperature dose not shows any effect on conversion. Hence, 90 °C was considered as optimum for the maximum % conversion.

The effect of base on the reaction is shown in the Fig. 6d. The study indicates that organic base triethyl amine (Et_3N) is less favorable for coupling reaction compare to that of inorganic base. The highest conversion was found in the case of K_2CO_3 and NaOH compared to Na_2CO_3. As K_2CO_3 is environmentally benign, easy to handle and non-hygroscopic in nature compared to NaOH, further study was carried out with K_2CO_3.

The effect of different solvents showed that in case of ethanol, highest conversion was achieved compare to acetonitrile and toluene. The results are in good agreement with reported one, stating that polar solvents tend to give the best results for coupling reaction. Hence, ethanol was selected as an appropriate solvent for further study.

Further the effect of solvent to water (EtOH: H_2O) ratio was also studied. It was seen from the obtained results that in all the cases, conversion in aqueous medium is better than neat solvents. In case of ethanol alone, the conversion is 53% only, this is because of insolubility of base in reaction mixture. In case of (9:1) mL and (8:2) mL ratios base solubility increases due to increase in water amount. Hence, conversion also increases. The same trend was found for (7:3) mL, (5:5) mL and (3:7) mL ratios. Further, with increase in water amount, conversion decreases due to low solubility of the substrates in water compared to ethanol. Hence, (3:7) mL ratio is optimized for further study. Thus, the presence of water which acts as co-solvent can accelerate the reaction towards high yield of the product. This is expected because, presence of water facilitates the easy ionization of K_2CO_3 and provides basic medium for the reaction. Similarly, under the optimized (3:7) mL ratio, reactions with (CH_3CN: H_2O) and (toluene: H_2O) were also carried out and 92% and 23% conversion was found respectively.

From the above study, the optimized conditions for the maximum % conversion (99) are: iodobenzene (1.96 mmol), phenylboronic acid (2.94 mmol), K_2CO_3 (3.92 mmol), conc. of Pd(0) (0.0192 mol%), EtOH:H_2O (3:7) mL, catalyst/substrate ratio (5215/1), TOF (10012 h^{-1}), 30 min, 90 °C.

Further, the obtained product was purified by column chromatography on silica gel with a mixture of ethyl acetate and petroleum ether as eluent. Isolated yield (96%) was found to be the same with the conversion (96%) found by GC.

Heck Coupling

The efficiency of the $PdPW_{12}/ZrO_2$ as catalyst was also studied towards the Heck coupling. Iodobenzene was selected as the ideal substrate for the reaction to optimize the different influential reaction parameters such as substrate to catalyst ratio (catalyst amount), time, temperature, base and solvent for highest product conversion (scheme 3).

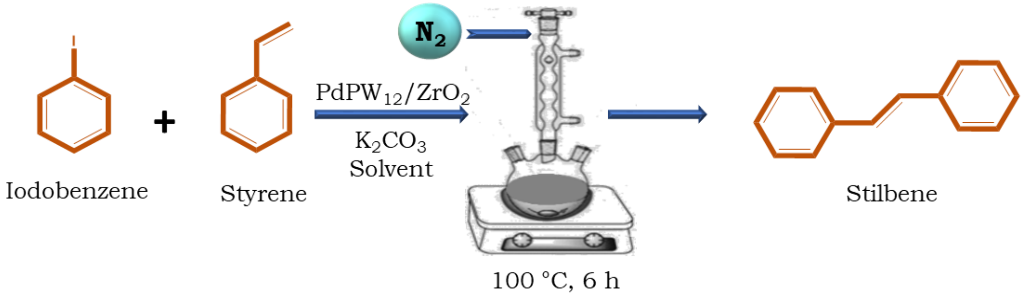

Scheme 3 Heck coupling.

Similar to SM coupling, the various reaction parameters such as effect of substrate/catalyst ratio, time, temperature, base, solvent and solvent ratio were studied and the optimized reaction parameters for the maximum % conversion (99) are: iodobenzene (0.98 mmol), styrene (1.49 mmol), K_2CO_3 (1.96 mmol), conc. of Pd(0) (1.06×10^{-3} mmol), DMF:H_2O (3:2) mL, Catalyst/Substrate ratio (1.08E-3), time (6 h), time (100 °C). The calculated turnover number (TON) is 860.

Further, the obtained product was purified by column chromatography on silica gel with a mixture of ethyl acetate and petroleum ether as eluent. Isolated yield (99%) was found to be identical with the conversion (99%) found by GC. The isolated product was identified by ^{1}H & ^{13}C NMR.

Hydrogenation

The efficiency of the $PdPW_{12}/ZrO_2$ as catalyst was also studied towards the hydrogenation. Cyclohexene was selected as the ideal substrate for the reaction to optimize the different influential reaction parameters such as substrate to catalyst ratio (catalyst amount), time, temperature, pressure and solvent for highest product conversion (scheme 4).

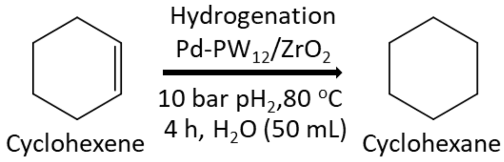

Scheme 4. Cyclohexene hydrogenation.

The effect of Pd concentration was evaluated by varying the catalyst amount from 10 to 25 mg (Substrate/Catalyst ratio from 26259/1 to 10504/1 respectively). Initially, with increase in concentration of Pd, % conversion also increases i.e. 10 mg to 20 mg (Figure 7a). Higher concentration of Pd would means a higher number of active sites to tolerate the substrate and gives higher conversion. With further increasing Pd concentration, the conversion remains constant. The highest, 99% conversion was achieved by 20 mg of catalyst.

Effect of temperature was screened from 60 to 90 °C and obtained results are presented in figure 7b. Results shows that % conversion increases with increase in temperature from 60 to 80 °C, as expected. Further increase in the temperature showed no effect on the % conversion.

Hydrogen pressure influence was evaluated and obtained results (Figure 7c) shows that with increase in pressure from 7 to 10 bar, the % conversion also increased linearly. Hence, the reaction is first order with respect to H_2 pressure. With further increase in pressure, no effect on the conversion was observed. Highest 94% conversion was obtained for 10 bar H_2 pressure.

The effect of time was investigated by varying the reaction time from 2 to 5 h (Figure 7d). It is seen from the results that initially with increase in time up to 4 h, the % conversion also increases, which is in good agreement with the well-known fact that as time increases, the formation of reactive intermediates from the reactant increases, and finally converted into the products. On further increasing the reaction time, the % conversion decreases. This might be due to occurrence of reversible process.

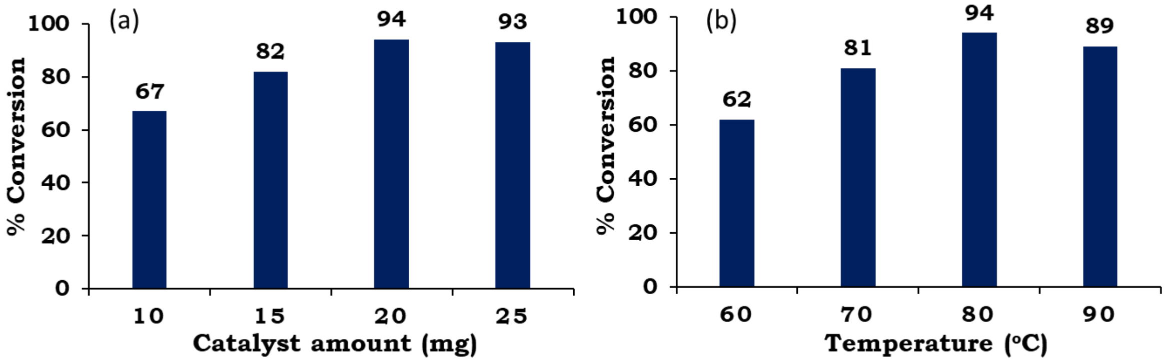

Cyclohexene (9.87 mmol), H_2O (50) mL, temperature (80 °C), H_2 pressure (10 bar), time (4 h).

Cyclohexene (9.87 mmol), H_2O (50 mL), catalyst (20 mg), H_2 pressure (10 bar), time (4 h).

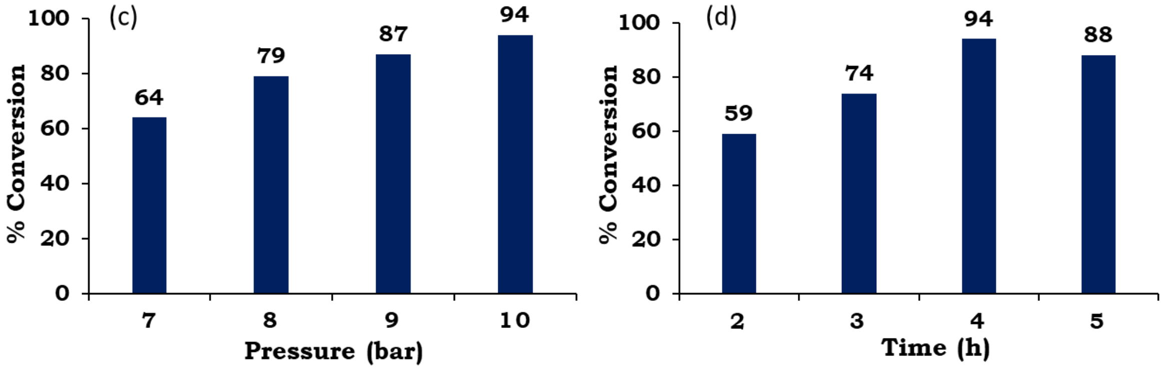

Cyclohexene (9.87 mmol), H_2O (50 mL), catalyst (20 mg), temperature (80 °C), time (4 h).

Cyclohexene (9.87 mmol), H_2O (50 mL), catalyst (20 mg), H_2 pressure (10 bar), temperature (80 °C).

Figure 7 Optimization of reaction parameters.

Effect of various solvents was studied and obtained results showed that comparatively, low % conversion was obtained in case of CH_3CN-H_2O solvent system due to its oxidizing nature which resists the reduction of cyclohexene. While it was achieved maximum for CH_3OH-H_2O, IPA–H_2O and CH_3OH-H_2O system and this may be due to their reducing nature. However, it was miracle that higher % conversion was obtained under the identical reaction conditions for neat water as a solvent (i.e. 96%). Hence, water was selected as a solvent for further study.

The optimized conditions for the maximum % conversion (94 are: cyclohexene (9.87 mmol), conc. of Pd(0) (0.015 mol%), H_2O (50 mL), H_2 pressure (10 bar), time (4 h) and temp. (80 °C), Substrate/Catalyst ratio (6565/1) and TON (6171).

For all three reactions, control experiments were carried out with $PdCl_2$, PW_{12} and $PdPW_{12}$ and ZrO_2 under optimized conditions. It is seen from the obtained results that PW_{12} and ZrO_2 are inactive towards the reaction. Almost same conversion was found in the case of $PdCl_2$, $PdPW_{11}$, and $PdPW_{11}/ZrO_2$. This indicates that Pd is real active species responsible for the reaction.

For all three reactions, heterogeneity and recyclability tests were carried out for $PdPW_{12}/ZrO_2$ by centrifuging the catalyst from the reaction mixture. This study also indicates that PW_{12} plays an important role in binding the palladium very strongly and thus does not allow the leaching of palladium into the reaction mixture, making it, a true heterogeneous catalyst to recycle and reuse up to five cycles without any appreciable change in activity.

Characterization of regenerated catalyst

In order to check the stability, the regenerated catalyst was characterized by elemental analysis (EDS), FT-IR and XPS.

EDS values of Pd (0.79 wt%) and W (16.32 wt%) of regenerated $PdPW_{12}/ZrO_2$ are in good agreement with values of fresh catalyst (0.80 wt% of Pd, 16.43 wt% of W) confirming no emission of Pd and PW_{12} from ZrO_2 during the reaction.

The FT-IR spectra (Figure 8) of the fresh and regenerated catalyst showed almost identical spectrum without any significant shift in characteristic bands of regenerated catalyst (R-$PdPW_{12}/ZrO_2$) compare to fresh catalyst, indicate that catalyst structure remained unaltered even after the regeneration.

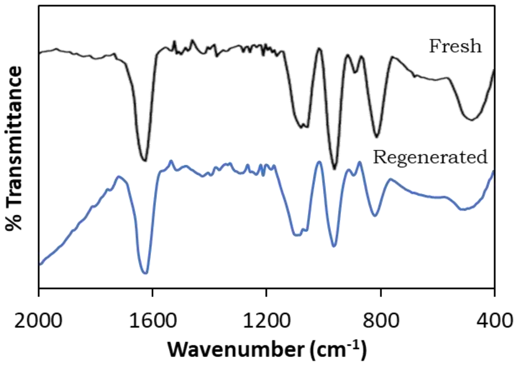

Figure 8 FT-IR spectra.

However, the spectrum was slightly different in terms of intensity. This might be due to the sticking of the substrates on the surface, although this might not be significant in the reutilization of the catalyst.

XRD of fresh and regenerated $PdPW_{12}/ZrO_2$ showed identical spectrum (Figure 9).

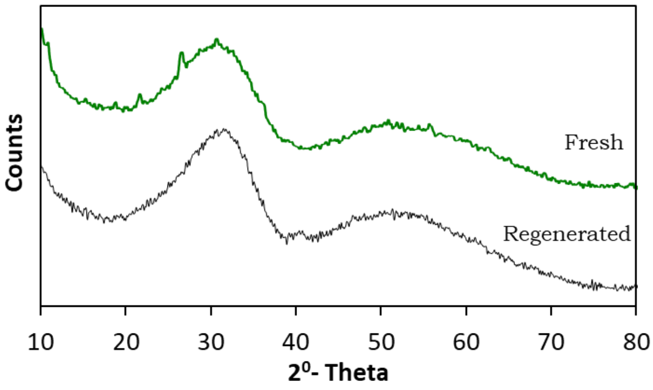

Figure 9 XRD spectra

The absence of any crystalline peaks confirms that there was no aggregates formation PdNPs as well as Keggin basic structure during the reaction, showcasing the sustainability of the catalyst under the optimized conditions.

Chapter 3: Zirconia Supported Stabilized PdNPs by mono lacunary tungstophosphate: Synthesis, characterization and applications for SM, Heck and hydrogenation

Palladium mono lacunary tungstophosphate was synthesized by direct method as reported in the literature[15] with modification. 1 g of Na_7PW_{11} was dissolved in minimum amount of distilled water followed by the addition of a stoichiometric amount of aqueous $PdCl_2$ (58.6 mg) solution dropwise. The resulting mixture was aged for 1 h at 80 °C and the excess water was evaporated to dryness on the water bath. The resulting material was oven dried at 120 °C overnight, calcined at 300 °C for 2 h to obtain brown coloured Na_5PdPW_{11}, designated as $PdPW_{11}$.

A series of materials, containing 10-40 % of $PdPW_{11}$supported on ZrO_2 was synthesized by incipient wet impregnation method. 1 g of ZrO_2 was impregnated with aqueous solution of $PdPW_{11}$ (0.1/10-0.4/40 g mL^{-1} of double distilled water) and dried at 100 °C for 10 h and finally treated under 1 bar H_2 pressure at 40 °C for 30 min using Parr reactor. The obtained materials with 10-40 % loading was designated as 10 % $PdPW_{11}/ZrO_2$, 20 % $PdPW_{11}/ZrO_2$, 30 % $PdPW_{11}/ZrO_2$ (Latter, $PdPW_{11}/ZrO_2$) and 40 % $PdPW_{11}/ZrO_2$ respectively.

The synthesized materials were characterized by elemental analysis (EDX), TGA, BET, FT-IR, XRD, XPS, TEM and HRTEM.

Elemental analysis shows the presence of all the expected elements, the found values for Pd (0.81 wt%) and W (14.82 wt%) are in good agreement with the theoretical values (Pd, 0.82 wt % and W, 14.90 wt%). FT-IR showed the presence of al the characteristic bands of PW_{11} in the synthesized material $PdPW_{11}/ZrO_2$, confirmed the retention of the kegging structure. The BET surface area was found to be 170 m^2 g^{-1}, whereas drastic increase was found for $PdPW_{11}/ZrO_2$ indicating the presence of Pd NPs. The N_2 sorption isotherm indicate the retention of the basic structure of the material even after loading. XRD pattern of the $PdPW_{11}/ZrO_2$ showed the absence of crystalline peaks corresponding to PdNPs as well as PW11, indicating the homogeneous dispersion of the PdNPs over the surface of the zirconia support. The XPS spectra indicates the presence of PdNPs as well as W in VI oxidation states, confirming no reduction of W(VI) during the synthesis of the materials. TEM images clearly shows the presence of PdNPs with homogeneous dispersion over the amorphous surface of the support.

The catalytic efficiency of the synthesized material was evaluated towards the SM, Heck and hydrogenation reactions and the preliminary study showed the following optimized parameters:

SM coupling: Iodobenzene (1.96 mmol), phenylboronic acid (2.94 mmol), catalyst (5 mg), K_2CO_3 (3.92 mmol), EtOH: H_2O (3:7) mL, temperature (90 °C), time (30 min).

Heck coupling: Iodobenzene (0.98 mmol), Styrene (1.47 mmol), catalyst (10 mg), K_2CO_3 (1.96 mmol), DMF: H_2O (3:2) mL, time (6 h), temperature (100 °C).

Hydrogenation: Cyclohexene (9.87 mmol), catalyst (15 mg), H_2O (50) mL, temperature (80 °C), H_2 pressure (10 bar), time (4 h).

Further optimization, control experiments, heterogeneity test and characterization of regenerated catalyst are in progress.

Part B:

Chapter 1: Stabilized PdNPs by zirconia supported 12-tungstophosphoric acid: Synthesis, characterization and applications for SM and hydrogenation

To design the catalyst, the advantage of available counter protons of zirconia supported 12-tungstophosphoric acid was exploited. Zirconia (ZrO_2)[21] and zirconia supported 12-tungstophosphoric acid (PW_{12}/ZrO_2) was synthesized by following the same method reported by us. Palladium (II) was deposited on supported 12-tungstophosphoric acid via exchanging the available protons of TPA[22]. 1 g of PW_{12}/ZrO_2 was soaked with 25 mL 0.05 M aqueous solution of $PdCl_2$ for 24 h with stirring. The solution was filtered, washed with distilled water in order to remove the excess of palladium and dried in air at room temperature. The resulting brown catalyst was designated as Pd(II)-PW_{12}/ZrO_2. Then, synthesized catalyst was charged in a Parr reactor under 1 bar H_2 pressure, at 40 °C for 30 min to reduce Pd(II) to Pd(0). After that the catalyst was removed from reactor and kept in air to attain the room temperature. The obtained black catalyst was designated as Pd-PW_{12}/ZrO_2. The same procedure was followed for the synthesis of Pd(0)/ZrO_2.

On the similar lines, as discussed in chapter 2, the synthesized material was characterized by elemental analysis (EDX), TGA, FT-IR, XPS, TEM, BET surface area and XRD.

The gravimetric analysis shows 0.4 %wt of Pd in Pd(II)-PW_{12}/ZrO_2 as well as elemental analysis by EDX also shows 0.4 %wt of palladium in Pd- PW_{12}/ZrO_2. The TGA of the Pd- PW_{12}/ZrO_2 shows the 13 % weight loss up to 150 °C due to the loss of adsorbed water molecules. No weight loss was observed up to 470 °C indicating the stability of the catalyst up to 470 °C.

The FT-IR spectrum of Pd-PW_{12}/ZrO_2 shows the characteristic bands at 824, 945 and 1056 cm^{-1} corresponding to stretching vibration for W-O-W, W=O and P=O but with significant shift, may be due to the change in the environment. Here, additional band corresponding to Pd-O band is not observed, this may be due to the merging of band with Zr-O.

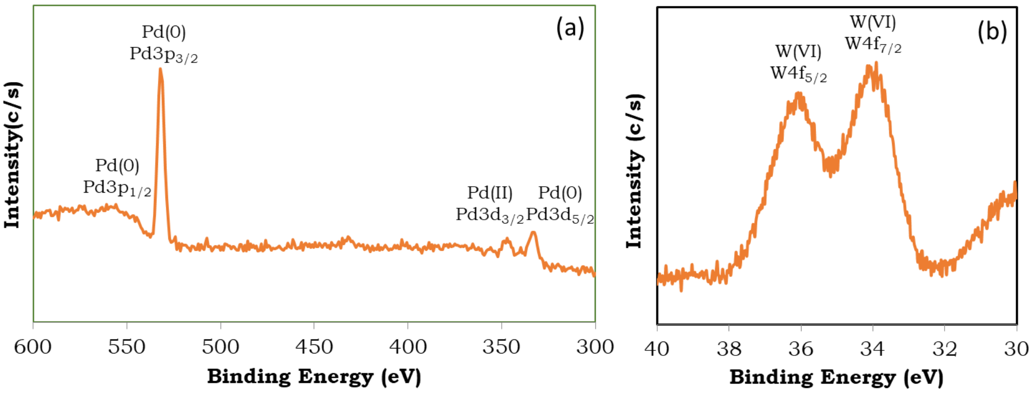

Figure 10 XPS of Pd-PW_{12}/ZrO_2

The X-Ray photoelectron spectrum of Pd-PW_{12}/ZrO_2 was recorded as shown in figure 10. A high intense peak at 532 eV ($3p_{3/2}$) is in agreement with reported one and confirms the presence of PdNPs on the surface. In addition, the peak obtained at 335 eV (3d5/2) as well as broad peak at 558 eV (3p1/2) also confirms the presence of PdNPs. However there are still a tiny number of Pd(II) present, as evidence by corresponding peak at 345.5 eV (3d3/2). From these obtained data and the intensities of the peaks, it is confirmed that amount of Pd(0) species is higher with a very trace amount of Pd(II) species in the catalyst. This is further confirmed by TEM.

SAED image indicates the non-crystalline and uniform distribution of Pd(0) in the synthesized catalyst. TEM images show the dark uniform suspension in the amorphous nature of the catalyst. This indicates the high dispersion of PdNPs over the surface of the catalyst.

The increase in surface area of the Pd(II)-PW_{12}/ZrO_2 (169 m^2 g^{-1}) as compared to that of PW_{12}/ZrO_2 (146 m^2 g^{-1}) indicates high uniform dispersion of the Pd on the surface of PW_{12}/ZrO_2. It is very interesting to note down that there is a drastic increase in the value of surface area of Pd-PW_{12}/ZrO_2 (203 m^2 g^{-1}) as compared to that of Pd(II)-PW_{12}/ZrO_2 (169 m^2 g^{-1}), conforming the reduction of Pd(II) to Pd(0) and in good agreement with the known fact that nanoparticles have higher surface area than the parent one.

The XRD patterns of PW_{12}/ZrO_2 and Pd-PW_{12}/ZrO_2 catalysts were recorded. The XRD pattern of TPA/ZrO_2 does not show any characteristic diffraction line indicating that a high dispersion of PW_{12} in a non-crystalline form on the surface of ZrO_2. In XRD patterns of Pd- PW_{12}/ZrO_2, absence of any crystalline peak corresponds to Pd(0), is due to the low concentration of Pd(0) on the surface of the catalyst as well as high dispersion of PdNPs on the surface of PW_{12}/ZrO_2.

Catalytic activity

The catalytic activity of the catalyst was evaluated towards SM and hydrogenation as mentioned in chapter 2, and the optimized conditions are as follows:

SM coupling: For maximum % conversion (99): Iodobenzene (1.96 mmol), phenylboronic acid (2.94 mmol), K_2CO_3 (3.92 mmol), conc. of Pd(0) (0.0096 mol%), EtOH:H_2O (3:7) mL, catalyst/substrate ratio (9.59E-5), TOF (20,642 h^{-1}), 30 min, 80 °C.

Hydrogenation: For maximum % conversion (96): Cyclohexene (9.87 mmol), conc. of Pd(0) (7.48×10^{-4} mmol), H_2O (50 mL), H_2 pressure (10 bar), time (4 h) and temp. (80 °C), Substrate/Catalyst ratio (13130/1) and TON (12,667).

To evaluate the efficiency of the catalyst for hydrogenation, crotonaldehyde was also selected as test substrates. Effect of different reaction parameters such as Pd concentration, solvent, temperature, pressure and time were studied to optimize the conditions for maximum conversion. As described in section of cyclohexene hydrogenation, in present case also, all parameters were varied. It should be noted that the explanation will remain the same as given in the section of cyclohexene hydrogenation (Figure 10). Here, in all the cases, butyraldehyde was obtained with 100% selectively. Whereas in case of EtOH: H_2O (20: 30) mL solvent system, we achieved 91% conversion with 60% butyraldehyde and 40% crotyl alcohol selectively.

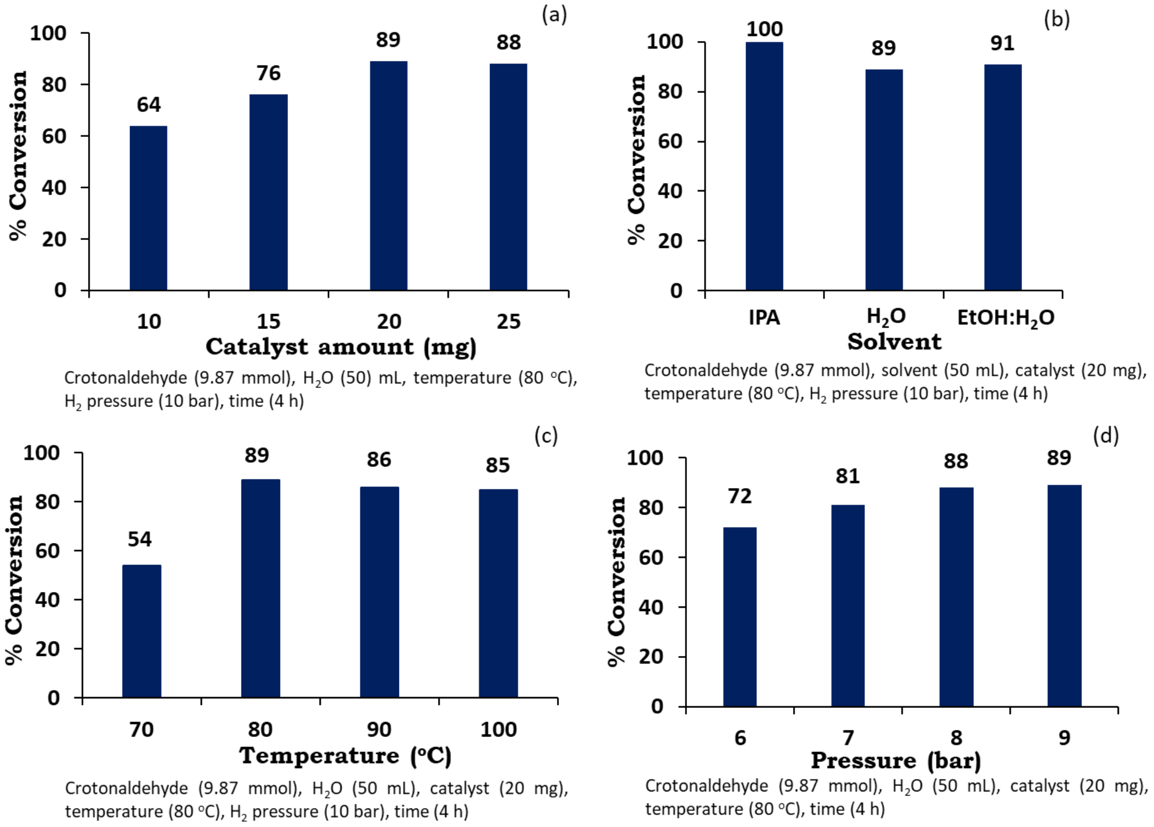

Crotonaldehyde (9.87 mmol), H_2O (50) mL, temperature (80 °C), H_2 pressure (10 bar), time (4 h)

Crotonaldehyde (9.87 mmol), solvent (50 mL), catalyst (20 mg), temperature (80 °C), H_2 pressure (10 bar), time (4 h)

Crotonaldehyde (9.87 mmol), H_2O (50 mL), catalyst (20 mg), temperature (80 °C), H_2 pressure (10 bar), time (4 h)

Crotonaldehyde (9.87 mmol), H_2O (50 mL), catalyst (20 mg), temperature (80 °C), time (4 h)

Figure 10 Optimization of reaction parameters.

The optimized conditions for the maximum % conversion (89) are: Crotonaldehyde (9.87 mmol), conc. of Pd(0) (7.48×10^{-4} mmol), H_2O (50 mL), temp. (80 °C), H_2 pressure (8 bar) and time (4 h). Substrate/Catalyst ratio (13130/1), TON (11744).

Control experiments for all the three reactions indicate that Pd is the real active species responsible for the reaction. Whereas leaching and recycling test confirms the no emission of PdNPs as well as PW_{12} from the support up to five catalytic runs. Heterogeneity test also confirms the true heterogeneous nature of the catalyst during the reactions.

Hydrogenation of crotonaldehyde gives three products selectively (i) Butyraldehyde (ii) Crotyl alcohol and (iii) *n*-butanol. It is well known that thermodynamic parameters favor the hydrogenation of C=C over the C=O bond[23] due to high activation energy of C=O tolerance to yield selectively butyraldehyde. However, C=O selectively can be reduced by either designing the suitable bimetallic catalyst or using organic solvent as discussed in introduction part. In the present work, we achieved single selective product that is butyraldehyde instead of product mixture. There might be two reasons for the selective reduction of C=C bond. (i) The presence of only water as a solvent instead of any organic solvent as discussed above. Here, the absence of organic solvent would not activate C=O bond to selectively produce butyraldehyde only. To check the same, we have carried out the same reaction under the optimized condition using EtOH: H_2O (20:30) mL as a solvent. Obtained results showed 91% conversion with 60% butyraldehyde and 40% crotylalcohol selectivity, indicating the activation of C=O bond for hydrogenation due to the presence of EtOH as solvent. (ii) The high adsorption capacity of the catalyst towards the substrates and initially formed products. In present case, initially formed product butyraldehyde got adsorbed on the surface of the catalyst, and did not allow it to desorb for further hydrogenation to generate other product butanol. Hence, we are expecting the well-known mechanism for both the reactions. The proposed mechanism is shown in scheme 5.

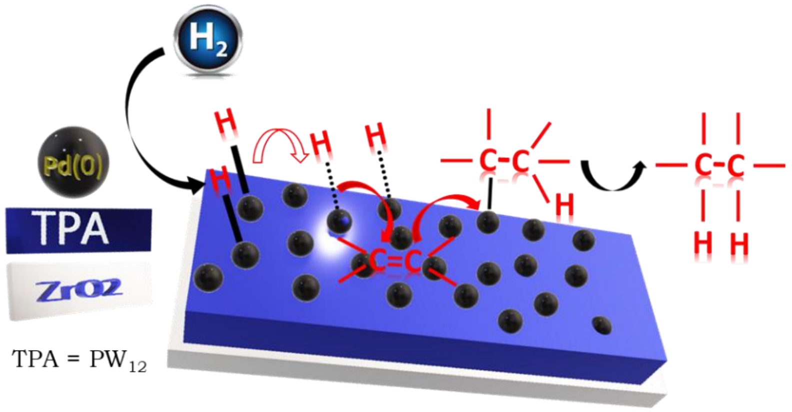

Scheme 5 Plausible mechanism.

Chapter 2: Stabilized PdNPs by zirconia supported mono lacunary tungstophosphoric acid: Synthesis, characterization and applications for SM, Heck and hydrogenation

Palladium was deposited on PW_{11}/ZrO_2 via exchanging the available protons of PW_{11}. 1 g of PW_{11}/ZrO_2 was soaked with 25 mL of 0.05 M aqueous solution of $PdCl_2$ for 24 h with stirring. The solution was filtered, washed with distilled water in order to remove the excess of $PdCl_2$ and dried in air at room temperature. The resulting (brown colored) material was designated as Pd(II)-PW_{11}/ZrO_2. Finally, the synthesized material was charged in a Parr reactor under 1 bar H_2 pressure, at 40 °C for 30 min to reduce Pd(II) to Pd(0). The obtained (black colored) material was designated as Pd-PW_{11}/ZrO_2.

The synthesized material was characterized by various physico-chemical techniques in which, gravimetric as well as EDX showed the presence of Pd was 0.72 % wt. FT-IR, ^{31}P MAS NMR and powder XRD combinedly indicated the retention of the Keggin unit even after exchange and reduction treatment. BET showed that presented material has very high surface area i.e. 213 $m^2\ g^{-1}$. N_2 sorption isotherms confirms the retention of the basic structure in the synthesized material. XPS confirmed the presence of Pd(0) and W(VI). Whereas, TEM indicated the sole presence of isolated PdNPs over the surface of the catalyst.

The catalytic efficiency of the catalyst was evaluated towards SM, Heck and hydrogenation reaction and optimized reaction parameters are as follows:
SM: For maximum % conversion (99): Iodobenzene (1.96 mmol), phenylboronic acid (2.94 mmol), K_2CO_3 (3.92 mmol), conc. of Pd (0.035 mol%), EtOH: H_2O (3:7) mL, catalyst/substrate ratio (14485/1), time (30 min), Temp (90 °C).

Heck: For maximum % conversion (96) are: Iodobenzene (0.98 mmol), styrene (1.49 mmol), K_2CO_3 (1.96 mmol), conc. of Pd (0.0207 mol%), DMF: H_2O (3:2) mL, Catalyst/Substrate ratio (483/1), time (6 h), temp (100 °C), TON (464).

Hydrogenation: For maximum % conversion (96) are: Cyclohexene (9.87 mmol), conc. of Pd (0.0034 mol%), H_2O (50 mL), H_2 pressure (10 bar), time (2 h) and temp. (50 °C) and Substrate/Catalyst ratio (29177/1), TON (28010) and TOF (14005 h^{-1}).
Control experiments for all the three reactions indicate that Pd is the real active species responsible for the reaction. Whereas leaching and recycling test confirms the no emission of PdNPs as well as PW_{11} from the support up to five catalytic runs. Heterogeneity test also confirms the true heterogeneous nature of the catalyst during the reactions.

In order to study the role of the support, we have chosen another acidic metal oxide-based support, SiO_2.

Annexure: Silica encapsulated Stabilized PdNPs by 12-tungstophosphoric acid: Synthesis, characterization and applications for SM, Heck and hydrogenation

A series of materials, containing 10-40 % of Pd(II)PW_{12} encapsulated in SiO_2 was synthesized by incipient wet impregnation method. 1 g of SiO_2 was impregnated with aqueous solution of Pd(II)PW_{12} (0.1/10-0.4/40 g mL^{-1} of double distilled water) and dried at 100 °C for 10 h and finally treated under 1 bar H_2 pressure at 40 °C for 30 min using Parr reactor. The obtained materials with 10-40 % loading was designated as 10 % PdPW_{12}/SiO_2, 20 % Pd PW_{12}/SiO_2, 30 % Pd PW_{12}/SiO_2 (Latter, Pd PW_{12}/SiO_2) and 40 % Pd PW_{12}/SiO_2 respectively.

The synthesized material was characterized by various physico-chemical techniques in which, gravimetric as well as EDX showed the presence of Pd was 0.80 % wt. FT-IR, ^{31}P MAS NMR and powder XRD combinedly indicated the retention of the Keggin unit even after encapsulation and reduction treatment. BET showed that presented material has very high surface area i.e. 322 m^2 g^{-1}. N_2 sorption isotherms confirms the retention of the basic structure in the synthesized material. XPS confirmed the presence of Pd(0) and W(VI). Whereas, TEM indicated the sole presence of encapsulated PdNPs inside the pores of the silica.

The catalytic efficiency of the catalyst was evaluated towards SM, Heck and hydrogenation reaction and optimized reaction parameters are as follows:
SM: For maximum % conversion (97): Iodobenzene (1.96 mmol), phenylboronic acid (2.94 mmol), K_2CO_3 (3.92 mmol), conc. of Pd (0.0192 mol%), EtOH: H_2O (3:7) mL, catalyst/substrate ratio (5215/1), TOF (10,116 h^{-1}), 30 min, 90 °C.

Heck: For maximum % conversion (99) are: Iodobenzene (0.98 mmol), styrene (1.49 mmol), K_2CO_3 (1.96 mmol), conc. of Pd (0.115 mol%), DMF: H_2O (3:2) mL, Catalyst/Substrate ratio (869/1), time (6 h), time (100 °C). The calculated turnover number (TON) is 860.

Hydrogenation: For maximum % conversion (97) are: Cyclohexene (9.87 mmol), conc. of Pd (0.023 mol%), H_2O (50 mL), H_2 pressure (8 bar), time (4 h) and temp. (50 °C) and Substrate/Catalyst ratio (4377/1), TON (4245) and TOF (1061 h^{-1}).

Control experiments for all the three reactions indicate that Pd is the real active species responsible for the reaction. Whereas leaching and recycling test confirms the no emission of PdNPs as well as PW_{12} from the support up to five catalytic runs. Heterogeneity test also confirms the true heterogeneous nature of the catalyst during the reactions.

Summary

Ligand free, stabilized, environmentally benign heterogeneous catalysts were designed based on supported 12-tungstophosphoric acid/mono lacunary tungstophosphoric acid and Pd. $PdPW_{12}$, $PdPW_{11}$, $PdPW_{12}/ZrO_2$, $PdPW_{11}/ZrO_2$ and $PdPW_{12}/SiO_2$ were synthesized by direct method whereas $Pd\text{-}PW_{12}/ZrO_2$ and $Pd\text{-}PW_{11}/ZrO_2$ were synthesized by exchanged method. All the synthesized materials were characterized by elemental analysis, TGA, FT-IR, powder XRD, BET, ^{31}P MAS NMR, XPS and TEM. Characterization of $PdPW_{11}$ and $PdPW_{11}/ZrO_2$ are in progress.

The efficiency of the synthesized catalysts were evaluated towards C-C coupling Suzuki-Miyaura and Heck) and hydrogenation reactions by varying various reaction parameters such as temperature, pressure, time, solvent and solvent ratio in order to achieve maximum reaction conversion and selectivity towards desired product. Whereas the same for $PdPW_{11}/ZrO_2$ is in progress.

For all the catalytic systems, the heterogeneity test and recycling tests were performed under optimized conditions, and the results showed the true heterogeneous nature of all the systems and can be used up to 5 catalytic runs and can be used for more. The same will be performed for the $PdPW_{11}/ZrO_2$ catalytic system. The regenerated catalysts were characterized by elemental analysis, FT-IR, BET, XPS and TEM confirmed the stability of the catalyst under optimized conditions.

The reaction mechanism for crotonaldehyde and cyclohexene reactions were investigated in case of $Pd\text{-}PW_{12}/ZrO_2$ and $PdPW_{12}/SiO_2$ systems respectively.

References

[1] Yu H, Xue Y, Huang B, Hui L, Zhang C, Fang Y, Liu Y, Zhao Y, Li Y, Liu H, Li Y, iScience, 2019, 11, 31-41.

[2] Xi J, Sun H, Wang D, Zhang Z, Duan X, Xiao J, Xiao F, Liu L, Wang S, Appl. Catal. B: Environ., 2018, 225, 291-297.

[3] Qiao B, Wang A, Yang X, Allard LF, Jiang Z, Cui Y, Liu J, Li J, Zhang T, Nat. Chem., 2011, 3, 634-641.

[4] Hackett SFJ, Brydson RM, Gass MH, Harvey I, Newman AD, Wilson K, Lee AF, Angew. Chem. Int. Ed., 2007, 46, 8593-8596.

[5] Kim Y-T, Ohshima K, Higashimine K, Uruga T, Takata M, Suematsu H, Mitani T, Angew. Chem. Int. Ed., 2006, 45, 407-411.

[6] Zhai Y, Pierre D, Si R, Deng W, Ferrin P, Nilekar AU, Peng G, Herron JA, Bell DC, Saltsburg H, Mavrikakis M, Flytzani-Stephanopoulos M, Science, 2010, 329, 1633.

[7] Zhang C, Liu F, Zhai Y, Ariga H, Yi N, Liu Y, Asakura K, Flytzani-Stephanopoulos M, He H, Angew. Chem. Int. Ed., 2012, 51, 9628-9632.

[8] Özkar S, Finke RG, Langmuir, 2016, 32, 3699-3716.

[9] Kogan V, Aizenshtat Z, Popovitz-Biro R, Neumann R, Org. Lett., 2002, 4, 3529-3532.

[10] D'Souza L, Noeske M, Richards RM, Kortz U, Appl. Catal. A: Gen., 2013, 453, 262-271.

[11] He P, Xu B, Xu X, Song L, Wang X, Chem. Sci., 2016, 7, 1011-1015.

[12] Li H, Sun H, Qi W, Xu M, Wu L, Angew. Chem. Int. Ed., 2007, 46, 1300-1303.

[13] Yin P, Li D, Liu T, Isr. J. Chem., 2011, 51, 191-204.

[14] Muto K, Yamaguchi J, Musaev DG, Itami K, Nat. Commun., 2015, 6, 7508.

[15] Kumar CR, Jagadeeswaraiah K, Prasad PSS, Lingaiah N, ChemCatChem, 2012, 4, 1360-1367.

[16] Mizuno N, Min J-S, Taguchi A, Chem. Mater., 2004, 16, 2819-2825.

[17] Leng Y, Zhang C, Liu B, Liu M, Jiang P, Dai S, ChemSusChem, 2018, 11, 3396-3401.

[18] Villanneau R, Roucoux A, Beaunier P, Brouri D, Proust A, RSC Adv., 2014, 4, 26491-26498.

[19] D’Souza L, Noeske M, Richards RM, Kortz U, J Colloid Interface Sci, 2013, 394, 157-165.

[20] Tan H-Z, Wang Z-Q, Xu Z-N, Sun J, Chen Z-N, Chen Q-S, Chen Y, Guo G-C, Catal. Sci. & Tech., 2017, 7, 3785-3790.

[21] Patel S, Purohit N, Patel A, J. Mol. Catal. A, 2003, 192, 195-202.

[22] Pathan S, Patel A, RSC Adv., 2012, 2, 116-120.

[23] Ruiz-Martínez J, Fukui Y, Komatsu T, Sepúlveda-Escribano A, J. Catal., 2008, 260, 150-156.

Anish Patel
Research Scholar

Prof. (Dr.) Anjali Patel
Research Supervisor

Prof. (Dr.) Anjali Patel
Offg. Head
Department of Chemistry